

where c is the speed of sound, given by

$$\omega_Q = cq. \quad (\text{A6})$$

From Eq. (4.14), we obtain

$$\begin{aligned} W_0 &= \sum_{Q'} \mu\beta\omega_{Q'}n_{Q'}(1+n_{Q'})V_{Q'}(Q) \\ &= \frac{1}{6(2MN)^{1/2}} \frac{\mu\beta}{c} \omega_Q^{1/2} \sum_{Q'} \gamma_{Q'}\omega_{Q'}^2 n_{Q'}(1+n_{Q'}) \\ &= \frac{1}{6(2MN)^{1/2}} \mu\beta \left(\frac{q}{c}\right)^{1/2} \frac{\alpha_v V}{Kk_B\beta^2}. \end{aligned} \quad (\text{A7})$$

In the last step, we have used the Grüneisen relation.¹¹ α_v is the volume-expansion coefficient, V is the volume of the crystal, and K is the compressibility. For our simple model in Sec. IV,

$$1/K = NMc^2/V. \quad (\text{A8})$$

Hence,

$$|W_0|^2 = cq(C_p/C_v - 1)/72\beta, \quad (\text{A9})$$

using¹²

$$C_p - C_v = \alpha_v^2 V/k_B\beta K. \quad (\text{A10})$$

¹¹ J. M. Ziman, *Electrons and Phonons* (Clarendon Press, Oxford, England, 1960), p. 154.

¹² F. Seitz, *Modern Theory of Solids* (McGraw-Hill Book Company, Inc., New York, 1940), p. 137.

Magnetic Field Dependence of the Microwave Surface Impedance of Superconducting Tantalum*†

R. GLOSSER‡

Department of Physics and Institute for the Study of Metals, University of Chicago, Chicago, Illinois

(Received 12 October 1966)

The changes in the superconducting surface resistance $\Delta R_S = R_S(H) - R_S(0)$ and reactance $\Delta X_S = X_S(H) - X_S(0)$ of Ta with applied magnetic field H have been measured at a frequency of 8.8 GHz, using a dielectric-resonator technique. The quantity ΔR_S is found to be positive for a reduced temperature $t = T/T_C$ just less than 1, negative for $0.70 < t < 0.98$, and positive again for $t < 0.70$, while ΔX_S is always positive with a peak at about $t = 0.97$, a broad minimum centered at $t = 0.85$, and a continuous rise for lower temperatures. The dependence of ΔR_S and ΔX_S on the angle γ between \mathbf{H}_{rf} , the microwave magnetic field, and \mathbf{H} with both fields in the sample plane is investigated. The magnitude of this dependence is found to be a function of t .

I. INTRODUCTION

UNEXPECTED effects in the dependence of the superconducting surface impedance on an applied magnetic field H were first observed by Pippard¹ in the course of his measurements of the variation of penetration depth λ with H . One striking feature he found was that the superconducting surface resistance R_S of tin decreased with increasing H for $0 < H \lesssim 0.5H_C$, where H_C is the thermodynamic critical field. The magnitude of this decrease is expressed by $\Delta R_S/R_N = [R_S(H) - R_S(0)]/R_N$, where R_N is the normal-state surface resistance. At 9.4 GHz it was measured to be less than 5% in a reduced temperature range $t = T/T_C$ of $\sim 0.7 < t < 0.98$. The quantity T_C is the critical temperature of a superconductor. Further investigations of this effect were made on tin by Fawcett,² Spiewak,^{3,4} Richards,⁵⁻⁷

Dresselhaus *et al.*,⁸ Douglass *et al.*,⁹ and Lewis.¹⁰ Observations of the magnetic field dependence of the surface impedance have also been made in indium,⁴ aluminum¹¹⁻¹⁴ and tantalum.^{15,16} The surface reactance X_S

Conference on Low-Temperature Physics, 1960, edited by G. M. Graham and A. C. Hollis (University of Toronto Press, Toronto, 1960), p. 333.

⁶ P. L. Richards, *Bull. Am. Phys. Soc.* **6**, 65 (1961).

⁷ P. L. Richards, *Phys. Rev.* **126**, 912 (1962).

⁸ M. S. Dresselhaus, D. H. Douglass, Jr., and R. L. Kyhl, in *Proceedings of the Eighth International Conference on Low-Temperature Physics, London, 1962*, edited by R. O. Davies (Butterworths Scientific Publications, Ltd., London, 1963), p. 328.

⁹ D. H. Douglass, Jr., M. S. Dresselhaus, and R. L. Kyhl, *Bull. Am. Phys. Soc.* **8**, 78 (1963).

¹⁰ R. T. Lewis, *Phys. Rev.* **134**, A1 (1964).

¹¹ R. Glosser and D. H. Douglass, Jr., in *Proceedings of the Ninth International Conference on Low-Temperature Physics, Columbus, Ohio, 1964*, edited by J. G. Daunt, D. V. Edwards, F. J. Milford, and M. Yaquab (Plenum Press, Inc., New York, 1965), Part A, p. 385.

¹² W. V. Budzinski and M. P. Garfunkel, in *Proceedings of the Ninth International Conference on Low-Temperature Physics, Columbus, Ohio, 1964*, edited by J. G. Daunt, D. V. Edwards, F. J. Milford, and M. Yaquab (Plenum Press Inc., New York, 1965), Part A, p. 391.

¹³ W. V. Budzinski and M. P. Garfunkel, *Phys. Rev. Letters* **16**, 1100 (1966).

¹⁴ W. V. Budzinski and M. P. Garfunkel, *Phys. Rev. Letters* **17**, 24 (1966).

¹⁵ Yi-Han Kao and J. I. Budnick, *Phys. Letters* **17**, 218 (1965).

¹⁶ R. Glosser and D. H. Douglass, Jr., *Bull. Am. Phys. Soc.* **11**, 88 (1966).

* Supported in part by the U. S. Army Research Office (Durham) and the Advanced Research Projects Agency.

† Submitted in partial fulfillment of the requirements for the degree of Doctor of Philosophy at the University of Chicago.

‡ Present address: Michelson Laboratory, U. S. Naval Ordnance Test Station, China Lake, California.

¹ A. B. Pippard, *Proc. Roy. Soc. (London)* **A203**, 210 (1950).

² E. Fawcett, thesis, University of Cambridge, 1955 (unpublished).

³ M. Spiewak, *Phys. Rev. Letters* **1**, 136 (1958).

⁴ M. Spiewak, *Phys. Rev.* **113**, 1479 (1959).

⁵ P. L. Richards, in *Proceedings of the Seventh International*

also may decrease with increasing H .^{3-7,17} These effects in R_S and X_S depend not only on temperature but also on crystal orientation,³⁻⁷ relative orientation of rf and applied magnetic fields,^{3-7,11,13,17,18} frequency of incident radiation,^{10,12-14,19} and impurity content.^{7,14} The temperature dependence of ΔR_S in those measurements where the negative shift is present has usually been consistent with the original picture obtained by Pippard¹ in that ΔR_S is positive very close to $t=1$, then goes negative over some intermediate temperature range, and at lower temperatures is again positive. Lewis¹⁰ has pointed out that the minimum in a plot of ΔR_S versus t for tin shifts to a lower temperature as the frequency is raised.

The behavior of the change of the superconducting surface reactance with magnetic field ΔX_S is more complicated. At frequencies greater than 8.7 GHz, ΔX_S is always seen to be positive^{1,9-10}; the results are consistent with the picture of a peak in ΔX_S near $t=1$, a minimum at intermediate t , and a rise again at low t . For the range of frequencies $170 \text{ MHz} < \nu < 3 \text{ GHz}$, ΔX_S may change sign once^{4,7} or even twice¹⁷ as the temperature increases. At much lower frequencies $\nu < 2 \text{ MHz}$ ΔX_S has always been seen to be positive.^{20,21}

The magnitudes of ΔR_S and ΔX_S are largest for \mathbf{H}_{rf} parallel to \mathbf{H} .^{4,7,11,13,16-18} However, up until now no experimental determination has been made of the explicit angular dependence of ΔR_S and ΔX_S .

Richards⁷ demonstrated that an impurity concentration of about 0.2% or greater caused the negative shifts of R_S and X_S to disappear in tin. He inferred from this that l/λ rather than ξ/λ is the more significant parameter in this effect, where l is the mean free path and ξ is the coherence length.

An explanation for these effects in the H dependence of R_S and X_S was first offered by Bardeen,²² who suggested that they may be due to "a counter flow of normal and superfluid components perpendicular to the surface in the penetration region."

A more detailed theory was developed by Dresselhaus and Dresselhaus²³ also using a two-fluid model. This theory predicts changes in sign of ΔR_S and ΔX_S , and it predicts that the maximum change in these quantities

occurs for \mathbf{H}_{rf} parallel to \mathbf{H} , which is what has been observed. However, it has been pointed out by Pippard¹⁹ and Richards⁵⁻⁷ that in order to get agreement with experiment, an extremely small effective mass must be assumed. In addition, Richards's results are in disagreement with this theory as to the sign of ΔX_S when the impurity content is large.

Lewis¹⁰ proposed that the existence of more than one energy gap in tin may be responsible for the negative change of R_S with increasing H . This is based on the experimental observation of a knee in a plot of R_S/R_N which occurs at a temperature coincident with that of the minimum of $\Delta R_S/R_N$. Lewis associated the knee with a second energy gap.

Maki²⁴ has treated the effect of the static magnetic field as a shift of the quasiparticle excitation energy and developed this idea using the technique of Abrikosov, Gor'kov, and Khalatnikov.²⁵ His results predict a change in sign of ΔR_S but not of ΔX_S . Explicit predictions are made of the angular dependence of ΔX_S at the high and low temperature extremes. However, the form of his results is such that direct comparison with experiment is extremely difficult in the important intermediate temperature region.

A qualitative discussion of the effect of H on the real part σ_1 of the surface conductivity of a superconductor has been given by Budzinski and Garfunkel.¹⁴ They also treat the effect of H as a shift in quasiparticle excitation energy and indicate how at high t and small ν this shift will cause a decrease in σ_1 by decreasing the peak of the density of states near the gap edge. This may in turn explain the decrease in R_S , provided that changes in the imaginary part σ_2 of the surface conductivity are small or cause changes in R_S of the same sign as caused by changes in σ_1 . This follows from the relation Budzinski and Garfunkel obtain, in which

$$R_S/R_N \approx (\sigma_1/\sigma_N)(\sigma_2/\sigma_N)^{-4/3}.$$

In this paper we present for the first time the results of a detailed investigation of the magnetic field dependence of the surface impedance of a superconductor other than tin. In particular, the temperature and angular dependences of ΔR_S and ΔX_S are examined in tantalum at 8.8 GHz. We relate these to results obtained in tin and aluminum and make comparisons with Maki's predictions.

II. EXPERIMENT

A. Sample

The tantalum sample was obtained from a single-crystal rod supplied by Materials Research Corporation, Orangeburg, New York. Orientation to within 1° was accomplished by the backreflection Laue method. A

¹⁷ B. D. Josephson, thesis, University of Cambridge, 1964 (unpublished).

¹⁸ In Refs. 11 and 16 this author erred in stating that the maximum change in ΔR_S occurs for $\theta=90^\circ$, where θ (now γ in this paper) is the angle between \mathbf{H} and \mathbf{H}_{rf} . As will be shown in this paper, the maximum effect occurs for $\theta=0^\circ$. The error was due to an incorrect assumption of the polarization of the resonator mode.

¹⁹ A. B. Pippard, in *Proceedings of the Seventh International Conference on Low-Temperature Physics, 1960*, edited by G. M. Graham and A. C. Hollis (University of Toronto Press, Toronto, 1960), p. 320.

²⁰ Y. V. Sharvin and V. F. Gantmakher, *Zh. Eksperim. i Teor. Fiz.* **39**, 1242 (1960) [English transl.: *Soviet Phys.—JETP* **12**, 866 (1961)].

²¹ R. A. Connell, *Phys. Rev.* **129**, 1952 (1963).

²² J. Bardeen, *Phys. Rev. Letters* **1**, 399 (1958).

²³ G. Dresselhaus and M. S. Dresselhaus, *Phys. Rev.* **118**, 77 (1960).

²⁴ K. Maki, *Phys. Rev. Letters* **14**, 98 (1965).

²⁵ A. A. Abrikosov, L. P. Gorkov, and I. M. Khalatnikov, *Zh. Eksperim. i Teor. Fiz.* **35**, 265 (1958) [English transl.: *Soviet Phys.—JETP* **8**, 182 (1959)].

wafer of elliptical cross-section 13 mm \times 9.5 mm and 0.76 mm thick was spark cut from the rod. The [111] axis was perpendicular to the face. The wafer was etched in a solution of HF and NH_4F ,²⁶ and electropolished in a solution of H_2SO_4 and HF.²⁷

In order to remove the interstitial impurities, both those introduced during etching and electropolishing and those originally present in the sample, the wafer was treated by a process similar to that used by Seraphim *et al.*,²⁸ in preparing tantalum wires. The wafer was heated to 2000°C in oxygen at 10^{-5} Torr for one hour to remove carbon as CO_2 , and then the temperature was raised to 2300°C and the sample outgassed at a pressure of 3×10^{-7} Torr for 6 h. A resistivity ratio $(\rho_{300} - \rho_{4.2})/\rho_{4.2}$ of about 200 was obtained. This value was found by determining the temperature at which surface superconductivity first appeared and comparing this with the results of Seraphim and Cornell,²⁹ who empirically relate this onset temperature with the resistance ratio. Such a value, while adequate for this type of experiment, is considerably less than values $\sim 10^4$ which others have obtained.²⁸ However, such high-resistivity ratios were obtained in 10-mil-diam wires which had not been etched or electropolished. Any attempt by us to outgas longer or at higher temperature would have caused deterioration of the surface. The final purity is thus compromised in order to maintain a polished surface. Nevertheless, a resistivity ratio of 200 corresponds to an impurity concentration of only about 10^{-2} at.%.³⁰ The results of Richards⁷ show that in Sn an impurity concentration this small has very little effect on the values of $\Delta R_S/R_N$ compared to the values in a pure metal. We assume these results applicable to our Ta sample.

B. Apparatus

Our microwave apparatus is similar to that described by Dresselhaus, Douglass, and Kyhl.⁸ It permits measurements of fractional changes in R_S and X_S of about one part in 10^4 . The measurable shift in X_S corresponds to detecting a shift in resonant frequency of about one part in 10^7 . The sample-mounting geometry is designed for measuring the dependence of surface impedance on γ , the angle between the rf and applied magnetic fields, with a resolution of better than 3° . Also it is possible, because of the plane geometry, to make a more direct investigation of the effect of crystal direction. This possibility was not exploited in these experiments, however.

²⁶ *Metals Reference Book*, edited by J. C. Smithells (Butterworths Scientific Publications, Ltd., London, 1962), 3rd ed., Vol. 1, p. 258.

²⁷ W. J. McG. Tegart, *The Electrolytic and Chemical Polishing of Metals* (Pergamon Press Ltd., London, 1959), 2nd ed., p. 68.

²⁸ D. P. Seraphim, J. I. Budnick, and W. B. Ittner III, *Trans. AIME* 218, 527 (1960).

²⁹ D. P. Seraphim and R. A. Connell, *Phys. Rev.* 116, 606 (1959); the filamentary structure they refer to is to be identified with the surface sheath.

³⁰ D. P. Seraphim, *Solid-State Electron.* 1, 368 (1960).

Rutile Resonator Technique

Measurements of small changes in the microwave surface impedance of a bulk metal require a technique which permits detecting small changes in the amplitude and phase of the microwave signal reflected from the sample. This is best accomplished by making the sample a part of a resonant system with as much of the loading as possible taking place in the sample itself. In this experiment, the Ta sample is coupled to a dielectric resonator. Such a resonator has been described by Okaya and Barash³¹ and by Yee³² in considerable detail. Here we simply observe that for an insulator such as rutile with a high dielectric constant ϵ' , practically all the radiation is reflected at the boundary with air, so that an appropriately shaped piece of this material may be made to resonate at a given frequency. For illustration purposes, a schematic of a possible field configuration for such a resonator in free space and with a superconducting load is shown in Fig. 1. The most useful feature to us of such a field configuration is that the magnetic field lines penetrate outside the resonator. We exploit this by placing the metal sample under investigation in contact with one face of the resonator. The effect of this mating is to bring H_{rf} into close contact with the sample, thus loading the resonator. The maximum loss in the

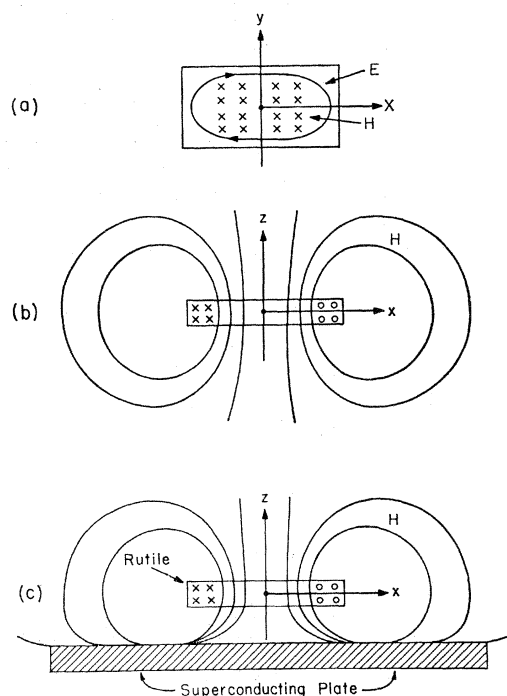


FIG. 1. Schematic of a possible electric and magnetic field configuration in a rutile dielectric resonator in free space (a), (b), and loaded by a superconducting plate in close proximity (c). Illustration adapted from Fig. 3 of Ref. 31 with permission.

³¹ A. Okaya and L. F. Barash, *Proc. I.R.E.*, 50, 2081 (1962).

³² H. Y. Yee, Microwave Laboratory, Report No. 1065, Stanford University, 1963 (unpublished).

sample in comparison with the dielectric losses in the resonator ranges from $R_N \sim R_D$ (which was the case in this experiment) to $R_N \sim 20R_D$ (as obtained by Dresselhaus *et al.*⁸). The quantity R_N is the normal-state microwave surface resistance, and R_D is an equivalent resistance corresponding to the dielectric loss. Any variations in the sample surface impedance are easily seen. This technique also permits a geometry favorable for interpretation of angular dependence, since the rf and applied magnetic fields may both be applied in the plane of the sample of some chosen orientation and angles between these fields and between these fields and the crystalline axes can be varied.

In the experiment, rutile (TiO_2) was used as the resonator material. It has an anisotropic dielectric constant of about 130 perpendicular to the optical axis and 250 parallel to it at liquid-helium temperatures.³³ This high dielectric constant made the dimensions of the resonator considerably smaller than the free-space wavelength, since $\lambda_D = \lambda_0 / \sqrt{\epsilon'}$, where λ_D is the wavelength in the dielectric and λ_0 that in free space. For measurements at 9 GHz, the resonator dimensions were 1 mm \times 4 mm \times 6 mm, with the optical axis along the 6-mm edge. The actual operating mode of the resonator was not determined, but this information was not needed, since we were only concerned with knowledge of the polarization of the microwave magnetic field and the relative orientation of it with respect to \mathbf{H} and the sample crystalline axes. This was determined experimentally by an electron-spin-resonance technique which we describe later.

Cryostat Assembly

This cryostat assembly is of standard design, with only one waveguide used for the incident and reflected microwaves for simplicity. The waveguide is cylindrical and propagates the circular TE_{11} mode. In the vicinity of the sample, it is made of No. 321 nonmagnetic stainless-steel tubing. Since we wish to avoid liquid He in the waveguide because it might mechanically disturb the resonance, we cool the sample with helium transfer gas. The geometry is shown in Fig. 2. The sample is attached to a microwave shorting choke with dots of General Electric 7031 varnish. The $[111]$ axis is perpendicular to the face of the sample and parallel to the waveguide axis. The rutile resonator is placed directly on top of the sample so that the microwave magnetic field is parallel to the $[211]$ axis. The resonator is held in position by a Styrofoam form. In order to measure sample temperature, a 1/10-W Allen-Bradley carbon resistor with a flattened surface is made to contact the bottom face of the crystal. The resistor is electrically insulated from the sample by a thin coat of General Electric 7031 varnish and thermally isolated from the

³³ E. S. Sabisky and H. J. Gerritsen, *J. Appl. Phys.* **33**, 1450 (1962).

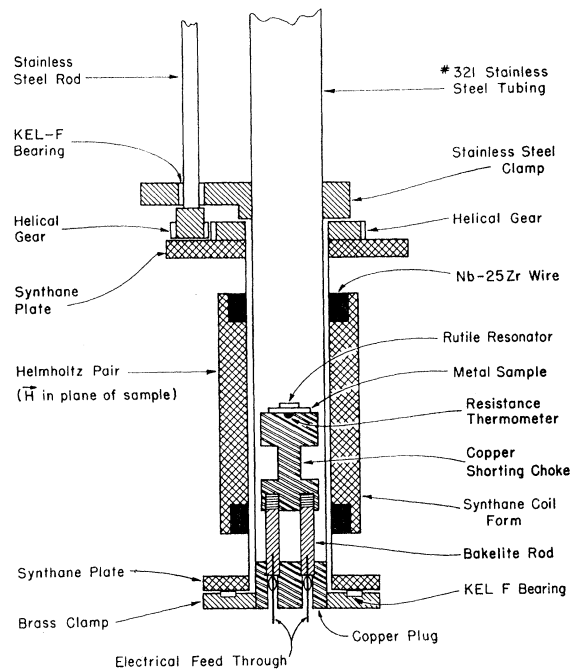


Fig. 2. Lower cryostat assembly showing the geometry of Ta sample and rutile resonator in the waveguide and the rotating magnet.

choke by a Bakelite form which also serves as the resistor mounting.

A magnetic field is applied in the plane of the sample by a Helmholtz pair, which may be rotated 360° about the sample. The mechanism is shown also in Fig. 2. The magnet was wound with Nb-25% Zr superconducting wire and was made to dimensions determined from tables prepared by Montgomery and Terrell,³⁴ in order to optimize the field homogeneity. The homogeneity was checked at room temperature with a Hall-probe Gaussmeter and was found to be better than 1% within a sphere of 13-mm. diam at the center of the magnet. The calibration was determined at 1.3°K by an electron-spin-resonance technique described in the experimental-technique section. The geometry factor was found to be 441.8 ± 1.3 G/A.

Microwave Apparatus

We wish to excite the loaded rutile resonator and observe the signals reflected from it. A schematic of how this is accomplished is shown in Fig. 3. The output of the signal klystron is divided equally between the signal arm and the reference arm of the microwave bridge. The portion of the signal klystron output in the signal arm is fed to a magic tee,³⁵ where it is divided

³⁴ D. B. Montgomery and J. Terrell, National Magnet Laboratory, Massachusetts Institute of Technology, Report No. AFOSR-1525, 1961 (unpublished).

³⁵ E. L. Ginzton, *Microwave Measurements* (McGraw-Hill Book Company, Inc., New York, 1957).

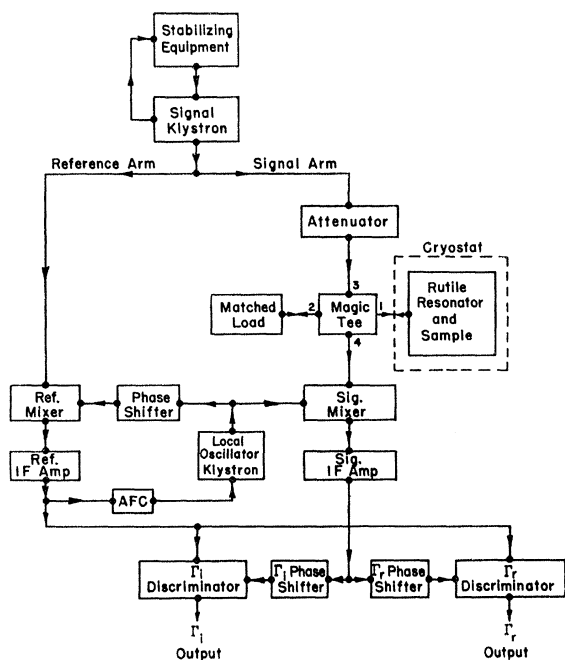


FIG. 3. Schematic of the microwave bridge.

between a matched load and the experimental load in the cryostat. The signal to the experimental arm is initially in the rectangular TE_{10} mode. It goes to a rectangular rotary joint and then into a rectangular to circular transition piece and finally into a circular rotary joint which mates with the cryostat circular waveguide. The result is that the plane of polarization of the TE_{11} circular-mode wave going to the experimental load may be rotated. This, plus an E - H tuner adjacent to the rectangular rotary joint, permits adjustment of coupling to the resonator. The microwave bridge is said to be balanced when the loaded resonator impedance is equal to the matched load impedance and thus to the waveguide impedance, so that no signal reaches port 4 of the magic tee.

Upon applying magnetic field, the impedance of the sample and hence that of the loaded resonator changes, and now a signal reaches port 4 of the magic tee. From here it goes to the signal mixer where it is combined with the local oscillator output to give a 30-MHz. signal. This is amplified and then divided equally between two phase-shifters labeled Γ_r and Γ_i . At the reference mixer, the signal-klystron output into the reference arm is combined with a portion of the local-oscillator output to give a 30-MHz reference which is coherent with the signal reflected from the experimental load. The reference is amplified and then divided between the Γ_r and Γ_i discriminators. The signal and reference are then compared in the two discriminators. The adjustments for this comparison are made in the following manner: The phase-shifter between the local-oscillator klystron and reference mixer is set so

that at resonance with some coupling other than critical (so that there is a reflected signal at resonance) there is a 45° phase shift between reference i.f. and signal i.f. Then, by using amplifiers detuned to the appropriate $\frac{1}{2}$ -power point, the signal i.f. is shifted by an additional -45° going into the Γ_r discriminator and $+45^\circ$ into the Γ_i discriminator. At resonance, the reference and signal are 90° out of phase in the Γ_i discriminator, and are in phase in the Γ_r discriminator. With these phase adjustments we then have, for any impedance of the loaded resonator, that the output of the Γ_i discriminator is $A\sin\phi$, while that of the Γ_r discriminator is $A\cos\phi$, where A is proportional to the amplitude of the reflected signal from the loaded resonator and ϕ is the phase angle between signal and reference. $A\cos\phi$ and $A\sin\phi$ with appropriate normalization are to be identified as the real and imaginary components of the reflection coefficient Γ , which is defined as the ratio of the amplitude of the reflected wave to the amplitude of the incident wave.³⁵ We discuss the normalization in Sec. III.

We may read out directly the changes in the impedance by plotting the discriminator outputs on Smith-chart coordinates.^{35,36} However, in practice we find it convenient to plot each output separately as a function of applied magnetic field with an x - y recorder on ordinary graph paper, or plot the outputs together, with either magnetic field H or frequency ν as a parameter, also on ordinary paper. The components of the impedance $\mathfrak{z} = \mathfrak{R} + j\mathfrak{X}$ may be obtained by plotting the normalized discriminator outputs Γ_r and Γ_i by hand on highly expanded Smith-chart paper or by calculation from the expression³⁷

$$\frac{\mathfrak{z}}{\mathfrak{z}_0} = \frac{1 - |\Gamma|^2 + j2\Gamma_i}{1 + |\Gamma|^2 - 2\Gamma_r},$$

where \mathfrak{z}_0 is the waveguide impedance.

The signal klystron is stabilized to a tunable reference cavity using standard discriminator and feedback techniques. The short-term frequency stability is estimated to be one part in 10^8 , while the long-term stability is about one part in 10^6 .

The local-oscillator klystron frequency is locked 30 MHz away from the signal-klystron frequency by using a small portion of the reference to generate an AFC (automatic frequency control)³⁸ signal which is then applied as feedback to the local-oscillator klystron power supply.

Thermometry

The sample thermometer's resistance was measured with a bridge built according to the design of Blake

³⁵ P. H. Smith, *Electronics* **12**, 29 (1939).

³⁷ *Principles of Microwave Circuits*, edited by C. G. Montgomery, R. H. Dicke, and E. M. Purcell (McGraw-Hill Book Company, Inc., New York, 1958), p. 72.

³⁸ F. E. Terman, *Electronic and Radio Engineering* (McGraw-Hill Book Company, Inc., New York, 1955), p. 953. The circuit used is a modified version of what is shown here.

and Chase.³⁹ The bath temperature above the lambda point was regulated by a diaphragm-type manostat similar to that described by Walker,⁴⁰ which could hold the sample temperature to within a millidegree over a period on the order of five minutes. Below the lambda point, temperature regulation was accomplished by a heater, controlled automatically by the thermometer bridge, so that the stability of the sample temperature was better than ten times that above lambda point.

Magnetic Field Control and Measurement

The magnet was driven by a programmable power supply which in turn was driven by an operational-amplifier-stabilized sweep circuit with variable sweep times. The magnetic field was determined by measuring the magnet current. The voltage across a 1- or 10- Ω resistor in series with the magnet drove the x axis of an x - y recorder in making plots of ΔR_S or ΔX_S versus H .

C. Experimental Technique

The reflection coefficient Γ of a resonant system, plotted on a Smith chart with frequency as a parameter, yields a circle usually referred to as a Q circle.³⁵ The tuning is adjusted so that the Q circle appears as shown in Fig. 4. This corresponds to critical coupling of the loaded resonator, which means that at resonance, the impedance of the experimental load is equal to that of the matched load and therefore no signal reaches port 4 of the magic tee.

The Q circle is plotted on the x - y recorder for normalization purposes, and then the klystron frequency is locked to the loaded resonator frequency with zero applied magnetic field. Starting from this balanced condition we plot the changes in surface resistance and reactance with H . The magnetic field is swept up to a desired maximum and back to zero to permit corrections for thermal drifts. Flux trapping in the sample was absent for H less than about $0.9 H_c$, above which the sample was in the intermediate state. Flux trapping in the magnet was not important as long as the magnet had not previously been operated at a much higher field than was needed for the immediate measurement.

The earth's magnetic field was not compensated or

shielded. Its contribution was taken into account near $t=1$ by observing the difference in magnet current, for opposite polarities, at which the sample would go normal. Also, the magnitude of earth's field and possible stray fields as well were measured in the vicinity of the sample. This information permitted a correction to be made to the field as obtained from the magnet current.

The angular dependence was obtained by rotating the Helmholtz pair and sweeping the field at various angles. The relative orientation of the rf magnetic field with respect to the static magnetic field was determined experimentally by use of the electron-spin-resonance (ESR) signal^{41,42} from the organic free-radical compound diphenylpicrylhydrazyl (DPPH). This was done in the final and separate run of this experiment in order to avoid any spurious effects. The DPPH was applied as a solution in benzene to the sample surface that was put in contact with the rutile. Upon evaporation of the benzene, the sample was left with a coating of the DPPH. The amplitude of the ESR is a maximum when the rf and applied magnetic fields are perpendicular, and it would be zero when the fields are parallel⁴² if the rf magnetic field were perfectly polarized. A ratio of maximum amplitude ($\gamma=90^\circ$) to minimum amplitude ($\gamma=0^\circ$) of about 3 was found for the ESR signal, but this does not accurately reflect the degree of polarization, since the resonance signals were so large that saturation effects in the electronics were important. However, the results of the angular dependence of $\Delta R_S/R_N$ at $t=0.940$ which we discuss in Sec. IV show a ratio of maximum to minimum magnitude that is at least 5.5. We believe this ratio represents the lower limit of the degree of polarization. The ESR technique also provided a means of calibrating the Helmholtz pair at liquid-He temperatures through the condition $h\nu = \beta g H$, for electromagnetic radiation inducing transitions between neighboring magnetic levels,⁴³ where h is Planck's constant, β is the Bohr magneton, and g is the spectroscopic splitting factor.

III. DATA ANALYSIS

It is convenient to normalize the superconducting surface impedance to the normal-state resistance, since absolute values are difficult to obtain. We show in the Appendix that

$$R_S/R_N = (1+f)Q_{0N}/Q_{0S} - f, \quad (1)$$

$$\frac{\Delta R_S}{R_N} = \frac{R_S(h) - R_S(0)}{R_N} = \frac{\Delta R}{\partial_0} (1+f) \frac{Q_{0N}}{Q_{0S}}, \quad (2)$$

and

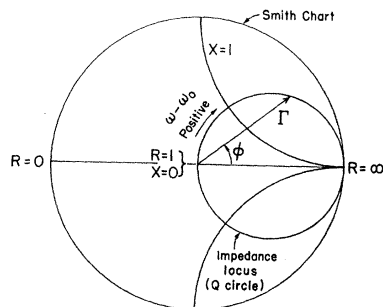
$$\frac{\Delta X_S}{R_N} = \frac{X_S(h) - X_S(0)}{R_N} = \frac{\Delta X}{\partial_0} (1+f) \frac{Q_{0N}}{Q_{0S}}, \quad (3)$$

⁴¹ T. L. Squires, *An Introduction to Electron Spin Resonance* (Academic Press Inc., New York, 1964), Chap. 1.

⁴² A. F. Kip, D. N. Langenberg, and T. W. Moore, *Phys. Rev.* **124**, 359 (1961). On page 367 a similar technique is described.

⁴³ C. Kittel, *Introduction to Solid State Physics* (John Wiley & Sons, Inc., New York, 1956), 2nd ed., p. 225.

FIG. 4. Smith Chart with a Q circle plotted for a critically coupled resonant system referred to the detuned open position. The complex reflection-coefficient vector Γ which describes the Q circle is shown.



³⁹ C. Blake and C. E. Chase, *Rev. Sci. Instr.* **34**, 984 (1963).

⁴⁰ E. J. Walker, *Rev. Sci. Instr.* **30**, 834 (1959).

where we now find it desirable to use the reduced magnetic field $h=H/H_c$. Here $\Delta R/\partial_0$ and $\Delta X/\partial_0$ are the changes in the resistance and reactance of the loaded resonator compared with the waveguide impedance ∂_0 , as determined by plotting Γ_r and Γ_i on Smith-chart coordinates. The discriminator outputs are normalized by dividing them by the Q -circle diameter to give Γ_r and Γ_i . We define $f=R_D/R_N$, which in this experiment has the value 0.99. The quantities Q_{0N} and Q_{0S} are the intrinsic Q 's of the loaded resonator with the tantalum in the normal and superconducting states, respectively. What is actually measured is the Q -circle diameter which is proportional to the loaded Q or Q_L , but for critical coupling we have $Q_L=Q_0/2$, so Q_{0N}/Q_{0S} is just the ratio of the diameters of the Q circles in the normal and superconducting states.

IV. RESULTS

The transition temperature for our tantalum sample was found to be $T_c=4.475\pm 0.004^\circ\text{K}$. This was deter-

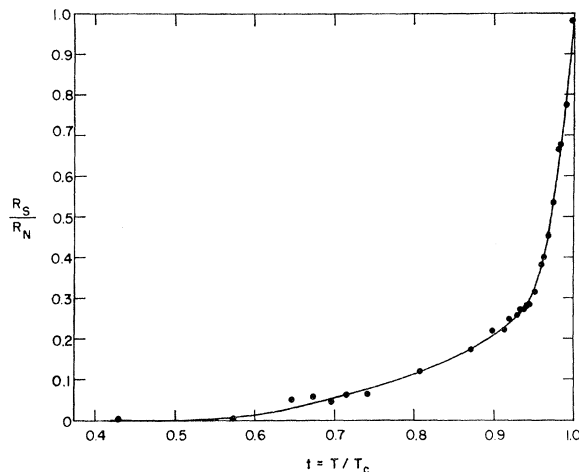


FIG. 5. Zero-magnetic-field temperature dependence of the superconducting surface resistance normalized to the normal-state surface resistance at 8.76 GHz.

mined by extrapolation of the critical-field-versus-temperature curve to zero field. The errors in t quoted below do not include the uncertainty in T_c .

The thermodynamic critical field H_c for $t > 0.807$ was obtained from the measurement of the magnet current corresponding to the field where the surface resistance first became independent of field. Corrections were made for the earth's field near $t=1$. Below $t=0.807$ the tantalum sample showed surface superconductivity, which meant experimentally that the large abrupt increase in resistance, instead of extending directly to the normal-state value R_N , ended at an intermediate value, and then, as H was further increased, the resistance rose gradually to R_N . We obtain H_c by extrapolating the abrupt increase to R_N which agrees

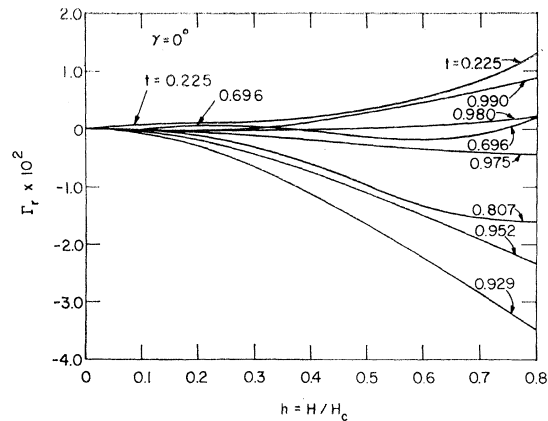


FIG. 6. Magnetic field dependence of the real part of the reflection coefficient Γ_r for various temperatures with \mathbf{H}_{rf} parallel to \mathbf{H} . The features are basically the same as for ΔR_S .

with Budnick's results.⁴⁴ There is the possibility of a systematic error in this procedure, according to the work on Pb by Fischer *et al.*,⁴⁵ where apparently the superconducting surface completely shields the interior to about 10% above H_c . They find that H_c is to be identified with the sharp break from the surface state into the intermediate state in decreasing field. If this were the case in our results, it would shift H_c down by no more than 2%, which is the difference in the sharp breaks between increasing and decreasing H , and this would have negligible influence on the results.

The temperature dependence of the zero-field surface resistance, as calculated from Eq. (1) is plotted in Fig. 5. Because of the possibility of a systematic

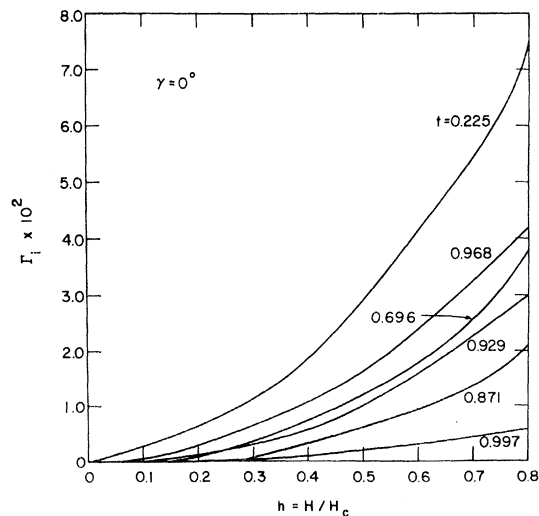
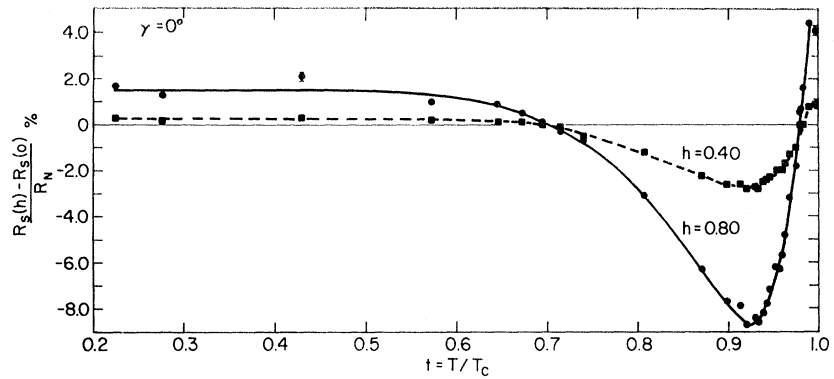


FIG. 7. Magnetic field dependence of the imaginary part of the reflection coefficient Γ_i for various temperatures with \mathbf{H}_{rf} parallel to \mathbf{H} . The features are basically the same as for ΔX_S .

⁴⁴ J. I. Budnick, Phys. Rev. **119**, 1578 (1960).

⁴⁵ G. Fischer, R. Klein, and J. P. McEnvoy, Solid State Commun. **4**, 361 (1966).

FIG. 8. Temperature dependence of $\Delta R_S/R_N$, with H_{rf} parallel to H for reduced fields of $h=0.80$ and 0.40 .

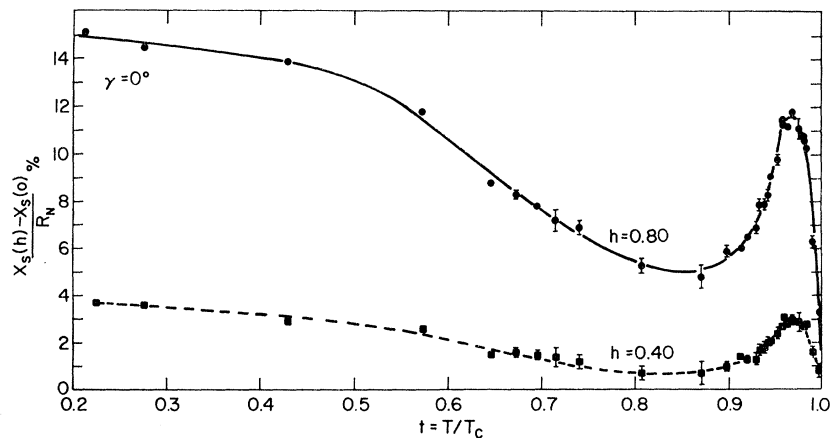


error in measuring the Q -circle diameter, there can be an uncertainty of as much as 20% in the plot of R_S/R_N as well as in the plots of $\Delta R_S/R_N$ and $\Delta X_S/R_N$. This uncertainty refers to a possible shift in the curves, but not in the relative values of the points. This possible Q -circle error is due to incomplete compensation for dispersion effects in the microwave bridge. Since our primary concern is about the relative changes in impedance, this error will not have an important effect on the basic features of the temperature dependence of $\Delta R_S/R_N$ and $\Delta X_S/R_N$.

The magnetic field dependence of Γ_r and Γ_i for $\gamma=0^\circ$ at various reduced temperatures is shown in Figs. 6 and 7. For these small changes in surface impedance, the features of Γ_r are practically the same as those of ΔR_S , and similarly for Γ_i and ΔX_S . The curves are averages of the discriminator output as plotted on the x - y recorder for increasing and decreasing H . In Fig. 6 we see ΔR_S change from positive to negative to positive as the temperature is lowered. At $t=0.696$ we note the sign change as a function of field. The positive change for low fields has an uncertainty which includes zero change, but around this temperature other curves of Γ_r seem to show that this small positive change is real and not due to temperature drift. For ΔX_S in Fig. 7 we note a rise, a decrease, and another rise as the tempera-

ture is lowered, but no change in sign. In Figs. 8 and 9, we show the temperature dependence of $\Delta R_S/R_N$ and $\Delta X_S/R_N$ for reduced-field values of $h=0.80$ and 0.40 with $\gamma=0^\circ$. In Fig. 8 we observe that very close to the transition temperature, $\Delta R_S/R_N$ is positive and is apparently peaked at some temperature between $0.990 < t < 0.997$. However, we do not observe an expected sharp rise from zero in $\Delta R_S/R_N$ at $t=1$ as was observed in tin by Lewis.¹⁰ As the temperature is lowered, there is a very sharp drop to negative values, with the crossover occurring at $t=0.980_{-0.002}^{+0.001}$ for $h=0.80$ and at $t=0.984_{-0.004}^{+0.000}$ for $h=0.40$. The minimum for $h=0.80$ is estimated to occur at $t=0.93$, and for $h=0.40$ it is at about $t=0.92$. The second crossing after a gradual rise is at $t=0.701 \pm 0.005$ for $h=0.80$ and at $t=0.695 \pm 0.01$ for $h=0.40$. Below these temperatures $\Delta R_S/R_N$ does not change very much with temperature, so that a best-fitting curve is essentially flat. In Fig. 9 we see that $\Delta X_S/R_N$ rises rapidly as the temperature is lowered and then peaks at about $t=0.97$ for both $h=0.80$ and 0.40 . The peaks are broad and the downturns are gradual, with minima around $t=0.85$ for $h=0.80$ and $t=0.83$ for $h=0.40$. For lower temperatures there is a slow but continuously rising change. In comparing $\Delta R_S/R_N$ with $\Delta X_S/R_N$, we note that the changes in $\Delta R_S/R_N$ are sharper than those of $\Delta X_S/R_N$,

FIG. 9. Temperature dependence of $\Delta X_S/R_N$, with H_{rf} parallel to H for reduced fields of $h=0.80$ and 0.40 .



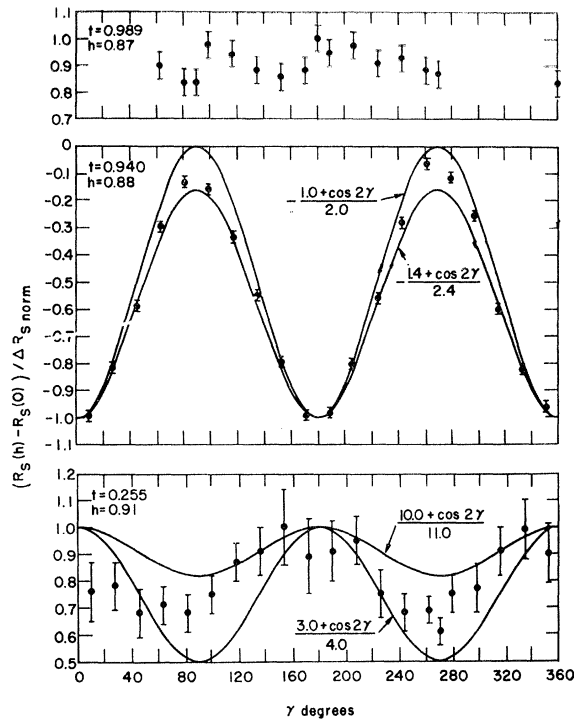


FIG. 10. Dependence of ΔR_S on γ , the angle between \mathbf{H}_{rf} and \mathbf{H} , for various temperatures at fixed magnetic fields. The number $\Delta R_{S \text{ norm}}$ is chosen to normalize the largest value of ΔR_S at each temperature to 1.

particularly in the high-temperature range. The peak on $\Delta X_S/R_N$ may be correlated with the crossover of $\Delta R_S/R_N$, but the separation seems to be more than 0.01 reduced-temperature units, so it may not be justified to tie them directly together.

The major source of uncertainty in the $\Delta R_S/R_N$ and $\Delta X_S/R_N$ points is due to temperature drifts of Γ_r and Γ_i while magnetic field was swept up and back. The nominal values are obtained by applying a linear correction for this drift, but sometimes this procedure would not be perfectly valid if the direction of drift were to change or were to start or stop in the course of the sweep. In any case the error bars give the maximum uncertainty. In the case of $\Delta R_S/R_N$ the error is relatively small, and except where error bars are present is within the size of the points. The change in reactance was more strongly affected by temperature drifts than the change in resistance, as can be seen by the larger error bars.

We have shown the temperature dependence of $\Delta R_S/R_N$ and $\Delta X_S/R_N$ for $\gamma=0^\circ$ because the magnitude of the changes is largest for this angle. We now consider how $\Delta R_S/R_N$ and $\Delta X_S/R_N$ vary as the angle is changed at fixed temperature. This is shown in Figs. 10 and 11. The changes in resistance and reactance are normalized at each temperature to values $\Delta R_{S \text{ norm}}$ and $\Delta X_{S \text{ norm}}$, which are chosen to make the largest value of each at a given temperature equal to 1. The variation of the

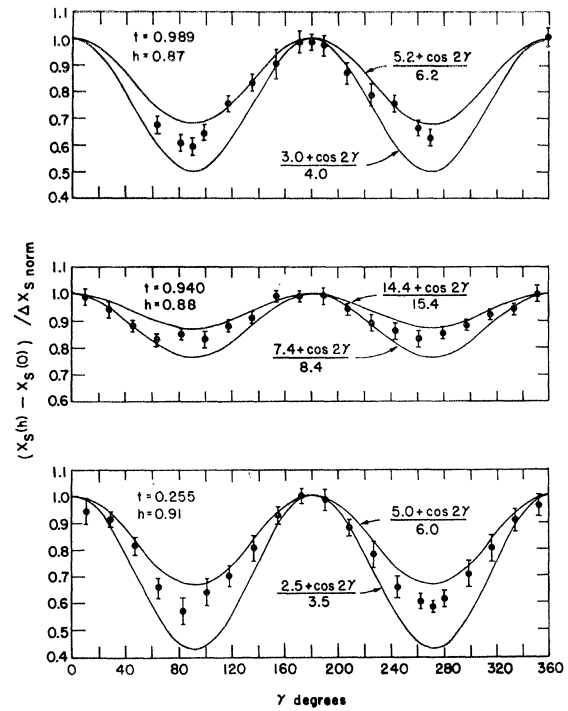


FIG. 11. Dependence of ΔX_S on γ , the angle between \mathbf{H}_{rf} and \mathbf{H} for various temperatures at fixed magnetic fields. The number $\Delta X_{S \text{ norm}}$ is chosen to normalize the largest value of ΔX_S at each temperature to 1.

demagnetization factor as \mathbf{H} was rotated was small but was allowed for.

The error bars again represent the uncertainty due to temperature drift. They do not include the variation in temperature from point to point. This we only bracket as being within ± 0.001 of the given reduced temperature.

Where possible, we bracket the angular variation of ΔR_S and ΔX_S by smooth cosine curves.

At $t=0.989$ we could not detect any angular variation in ΔR_S , as shown in Fig. 10, to within the temperature-stabilizing and noise limits of our system. The points at 90° , 180° , 270° , and 360° were taken in succession with a maximum temperature shift between these points, of ± 0.0005 . On the other hand, we have a sizable angular variation of ΔX_S at this temperature, as is seen in Fig. 11. We bracket the data by two cosine curves. The upper curve takes into consideration the error bars at $\gamma=90^\circ$ and 270° and the immediate vicinity. The lower curve also takes into consideration the error bars, but in addition includes an allowance for an enlargement of the angular dependence if \mathbf{H}_{rf} were perfectly plane polarized, since a degree of polarization of 5.5 is only a lower limit.

At $t=0.940$, where ΔR_S is strongly negative, we see that the angular dependence of ΔR_S is now very strong. In fact, its ratio of maximum to minimum provides our estimate of the degree of polarization of \mathbf{H}_{rf} . Since ΔR_S

TABLE I. Comparison of major features in plots of ΔR_s versus t and ΔX_s versus t for Sn, Ta, and Al at various frequencies. \mathbf{H}_{rf} is parallel to the applied \mathbf{H} .

Investigator	Element	ν GHz	ΔR_s			ΔX_s	
			Low-temperature crossover	Minimum	High-temperature crossover	Minimum	High-temperature maximum
Spiewak expt.	Sn (#1)	1	$t=0.97$	$t>0.97$...	$t \geq 0.97$	
Maki prediction			0.90		$t=0.998$		
Richards expt.	Sn [100]	3	0.68	≥ 0.8	...	≥ 0.90	
	Sn [110]	3	0.88	≥ 0.95	...	≥ 0.95	
	Sn [001]	3	0.90	≥ 0.95	...	≥ 0.95	
Maki prediction			0.90		0.996		
Present expt.	Ta	8.76	0.70	$=0.925$	0.980	$=0.85$	$t=0.97$
Maki prediction			0.91		0.988		
Glosser-Douglass	Al	8.87	...		0.96		
Maki prediction			0.89		0.957		
Douglass <i>et al.</i> expt.	Sn (001)	9			0.98		
Maki prediction					0.987		
Dresselhaus <i>et al.</i> expt.	Sn (101)	9.4	0.8				
Maki prediction			0.9				
Pippard expt.	Sn	9.4	0.70	...	0.976	0.83	≥ 0.97
Maki prediction			0.90		0.986		
Lewis expt.	Sn	23.5	0.7	$=0.88$	0.93	0.77	$=0.92$
Maki prediction			0.90		0.967		

is negative, the lower cosine curve is determined by the lowest error bar, while the upper curve, being $(1 + \cos 2\gamma)/2$, is just the upper limit if \mathbf{H}_{rf} were perfectly polarized.⁴⁶ At this temperature, ΔX_s has a smaller angular dependence than at $t=0.989$ by a factor of about 0.7.

At a low temperature of $t=0.255$, the magnitude of the ΔR_s angular dependence is small again but still observable. ΔX_s shows an angular variation quite similar to that found at $t=0.989$.

V. DISCUSSION

Our results for the temperature dependence of ΔR_s and ΔX_s in Ta at 8.8 GHz fit in very well with the results found by others in Sn. This in itself is significant, since it is the first time that such a detailed investigation of the H dependence of the surface impedance has been made on a material other than Sn with a view toward examining ΔR_s and ΔX_s as a function of temperature and angle γ . That the results in Sn and Ta do seem to mesh and that the results in Al are consistent with these, as indicated in Table I, adds justification for a theory such as Maki's,²⁴ which predicts qualitatively at least much of the behavior observed in ΔR_s and ΔX_s by relying only on the microscopic theory of superconductivity and not on any specific model of the band structure of a metal. In other words, we do not believe that negative shifts in ΔR_s and ΔX_s can be accounted

for by a theory in which multiple gaps in superconductors arise from separate bands between which there is little scattering compared to that within a band.^{10,47} It is difficult to see how a theory dependent on band structure can account for the similarity of phenomena observed in four metals with dissimilar band structures. This is not to say that band structure plays no part in these effects. The results of Richards⁷ show a dependence of ΔR_s and ΔX_s on crystal orientation, which is probably a result of energy-gap anisotropy. This we believe is a modification of the behavior of the surface impedance in a magnetic field, but not the cause.

The theory by Maki, while capable of predicting this similarity of phenomena, is not completely successful, and we will attempt to bring out both the successes and the failures of the theory in the following discussion.

In Table I, we compare the prominent features of the temperature dependence of ΔR_s and ΔX_s in Sn, Al, and Ta, as found by various investigators^{1,4,7-11} and as predicted by Maki.²⁴ In the table we compare only the results when \mathbf{H}_{rf} is parallel to \mathbf{H} , since then the effect is larger and more results are available.

Although Spiewak⁴ and Richards⁷ did not get to temperatures sufficiently close to $t=1$ to observe a minimum in ΔR_s and ΔX_s , we assume that one exists and we show the lower limit in Table I. We reason, as did Lewis,¹⁰ that at $t=1$ the critical field must be zero and therefore ΔR_s and ΔX_s must be zero. The theoretical reduced temperatures where ΔR_s changes sign (crossover temperatures) are obtained from the relations given by Maki.²⁴ He predicts that the low-temperature crossover will occur for $\Delta \sim kT$, where Δ is the superconducting energy gap and k is the Boltzmann constant. The high-temperature crossover is determined by the

⁴⁶ We assume that ΔR_s would not go positive for $\gamma=90^\circ$ if \mathbf{H}_{rf} were 100% linearly polarized. This we believe is valid on the basis of Richards's results (Ref. 7), where he has circularly polarized \mathbf{H}_{rf} so that with \mathbf{H} parallel to his sample axis, \mathbf{H} is unambiguously perpendicular to \mathbf{H}_{rf} . For \mathbf{H} either parallel or perpendicular to the sample axis, Richards observes ΔR_s negative for both cases in the same temperature range except possibly very close to the crossover temperature. In our experiment, at $t=0.94$ we are well away from the crossover temperature.

⁴⁷ H. Suhl, B. T. Matthias, and L. R. Walker, Phys. Rev. Letters **3**, 552 (1959).

condition $\Delta \sim (h\nu kT)^{1/2}$, where h is Planck's constant and ν is the frequency of the incident radiation. Here we assume these predictions to be equalities and compare them with the experimentally observed crossovers. The energy gap at zero temperature, $2\Delta(0)/kT_c$, is taken to be 3.6 for Ta, 3.5 for Sn, and 3.3 for Al. These values are averages of experimental values as quoted by Douglass and Falicov.⁴⁸ The temperature dependence of the gap is taken from the results of Mühlischlegel.⁴⁹

The low-temperature crossover for ΔR_S is practically the same for our results in Ta and for those of Pippard and Lewis in Sn despite the large range of frequencies. On the other hand, the results of Richards, Spiewak, and Dresselhaus *et al.*, show a range of values from $t=0.68$ to 0.97 .

This all might be considered consistent with the predicted crossover given by $\Delta \sim kT$ if we assume that the variation in this lower crossover temperature is due just to energy-gap variation. This is certainly possible, since the maximum and minimum values for energy gaps in Sn may differ by about 30%.

The high-temperature crossover for ΔR_S shows t decreasing as ν increases for the results where $\nu > 8$ GHz. The results of Spiewak and of Richards at $\nu < 8$ GHz are consistent with this behavior if we assume that they did not get close enough to $t=1$ to observe a second crossing. The shift of the high-temperature crossover is also in qualitative agreement with Maki's prediction. In Table I the prediction is given to three places, only to show this trend. To test if the relation $\Delta^2 \sim h\nu kT$ gives the predicted dependence, we compare the quantity $M = \Delta^2/\nu T$ for the results in tin by Pippard and by Lewis, where this crossover temperature is obtained and differs along with ν by a sizable amount. The values for M agree to within 20%, which is about all that could be expected given the theory in its present form and the uncertainty in the values of the energy gap at $t=0$.

Pippard¹⁹ quotes Fawcett's² results for ΔR_S in tin at $t=0.95$ and $\nu=35$ GHz. Here ΔR_S is found to be positive with \mathbf{H}_{rf} parallel to \mathbf{H} . This is to be expected, since the crossover temperature is calculated to be $t=0.952$; and since the experimental values are consistently lower than the calculated ones, ΔR_S should be positive at $t=0.95$ on this basis. It is unfortunate that it was not stated how low in temperature measurements were made on ΔR_S , since we might expect ΔR_S to be negative at some lower t . On the other hand, Budzinski and Garfunkel¹² see ΔR_S positive in Al at $t=0.84$ with $\nu=25$ GHz. At this t , we might expect ΔR_S to be negative. A possible explanation for these cases is simply that at these high frequencies with t large and

$H \sim H_c$, the photon energy is great enough to destroy Cooper pairs⁵⁰ so that any mechanism which tends to make ΔR_S negative is overshadowed. This would be expected to occur for smaller ν in Al than in Sn, since Al has a smaller gap (in energy units) than Sn. This is consistent with what has been observed.

At $\nu=8.9$ GHz it is found¹¹ that ΔR_S is negative in Al for $0.87 < t < 0.96$, where 0.87 was the lowest temperature reached. The high-temperature crossover for Al is consistent with the results in Sn and Ta and in agreement (although to some extent fortuitous) with Maki's prediction.

Lewis¹⁰ examined the frequency dependence of the minimum in the ΔR_S versus t plot, and found a behavior similar to that of the high-temperature crossover. Lewis plots $h\omega/kT$ versus t (his Fig. 15); for our results in Ta, we have $h\omega/kT \approx 0.1$ and $t_{\min}=0.925$, which falls close to the value expected from the smooth curve fitted to the other experimental values for Sn.

The general behavior of ΔX_S as a function of t seems to show a striking change in the frequency range between 3 and 8 GHz. For $\nu > 8$ GHz, ΔX_S in Sn and Ta has always been observed to be positive with very similar features in all cases. (Pippard actually considered $\Delta\lambda/\lambda$ but the features are equivalent⁴ to those of ΔX_S .) From Table I we see that both the minimum and the high-temperature maximum of ΔX_S versus t shift to lower t as the frequency is raised.

For $\nu < 3$ GHz, the picture is different. In the case that \mathbf{H}_{rf} is parallel to \mathbf{H} , the results of Spiewak⁴ and Richards⁷ show ΔX_S is negative for t near 1, becomes positive for $0.7 < t < 0.9$, and stays positive down to about $t=0.3$. Josephson¹⁷ finds a similar picture for Sn at $\nu=174$ MHz (he also considers $\Delta\lambda/\lambda$), but at around $t \sim 0.4$, the change in reactance becomes negative again.

When \mathbf{H}_{rf} is perpendicular to \mathbf{H} , Josephson and Spiewak observe ΔX_S to always be positive, while for three orientations, Richards observes only one case where ΔX_S goes negative.

Two experiments were done at low frequencies on the field dependence of λ . Sharvin and Gantmakher²⁰ found $\Delta\lambda$, and thus ΔX_S , positive in single-crystal Sn for \mathbf{H}_{rf} both parallel and perpendicular to \mathbf{H} at a frequency of 2 MHz. At 700 kHz, Connell²¹ also found $\Delta\lambda$ positive in polycrystalline Sn and In with the magnetic fields parallel.

Theoretically, according to Maki, ΔX_S is predicted to be always positive; but as we have seen, this seems to be only true for $\nu > 8$ GHz and at very low frequencies.

The behavior of the angular dependence of ΔR_S and ΔX_S with temperature is rather surprising. Most significant is the strong correlation between the sign of ΔR_S and the relative magnitudes of the angular dependences of ΔR_S and ΔX_S : When ΔR_S is negative, its γ dependence is strong, while that of ΔX_S is relatively

⁴⁸ D. H. Douglass, Jr. and L. M. Falicov, in *Progress in Low-Temperature Physics*, edited by C. J. Gorter (North-Holland Publishing Company, Amsterdam, 1964), Vol. 4, p. 97.

⁴⁹ B. Mühlischlegel, *Z. Physik* **155**, 313 (1959).

⁵⁰ L. N. Cooper, *Phys. Rev.* **104**, 1189 (1956); J. Bardeen, L. N. Cooper, and J. R. Schrieffer, *ibid.* **108**, 1175 (1957).

weak; and the opposite holds for the temperatures where ΔR_S is positive.

The form of the dependence of ΔR_S and ΔX_S on γ follows from general considerations. It is assumed that surface impedance can be defined independent of the rf field amplitude. From this it follows, neglecting crystalline anisotropy, that the angular dependence of both ΔR_S and ΔX_S is of the general form $(a+b \cos 2\gamma)$, since the surface impedance must be a 2×2 Hermitian matrix. Maki has predicted that the angular dependence of ΔX_S should go as $1+\cos 2\gamma$ at low temperatures ($\Delta \gg kT$) and should go as $2+\cos 2\gamma$ at higher temperatures ($\Delta \ll kT$). Our results in Fig. 11 are possibly consistent with the prediction that the γ dependence is stronger at the low-temperature extreme than at the high-temperature extreme. However, experimentally this is a slight effect, while theoretically it should be much larger. In addition, Maki's predictions lie outside the bracketing of the experimental points at both temperature extremes. There is a possibility that the inequalities he gives are here not sufficiently satisfied experimentally. At $t=0.989$, we have $\Delta(T)/kT \approx 0.3$, while at $t=0.255$ we have $\Delta(T)/kT \approx 7$. Maki also states that the γ dependence of ΔR_S should be similar to that of ΔX_S , but we observe this to be true only for the phase.

Any effect due to crystalline anisotropy with respect to \mathbf{H} was too small to be seen in our measurements of the angular dependence of the surface impedance. Since the crystal face was parallel to the (111) plane, which is threefold symmetric, and since \mathbf{H} was in the sample plane, the actual anisotropy would be sixfold symmetric with respect to \mathbf{H} . That is, a sign reversal of \mathbf{H} would not change anything as far as the impedance is concerned. Any anisotropy effects would appear in the curves of ΔR_S and ΔX_S versus γ as some modulation with a 60° period, and we see no indication of this in Figs. 10 and 11.

In summary, then, our results for the temperature dependence of ΔR_S and ΔX_S in Ta correspond very well with that of Sn in the same frequency range or higher, and fit in well with the qualitative predictions of Maki. Our results in Ta, as well as those obtained earlier in In⁴ and Al,¹¹ give strong support to the notion that the anomalous changes in surface impedance with H can be accounted for by a universal model of superconductivity. The sample geometry used in this experiment has for the first time permitted an investigation of the dependence of both ΔR_S and ΔX_S on γ without demagnetization effects being important.

The theoretical calculation seems to be successful in predicting the qualitative behavior of the temperature dependence of ΔR_S and the sign of ΔX_S above 8 GHz. Still to be predicted are the apparent sign change of ΔX_S between 2 and 174 MHz. and between 3 and 8 GHz, and the peculiar γ dependence of ΔR_S and ΔX_S with respect to each other and to temperature.

Of course, a quantitative description of ΔR_S and ΔX_S versus temperature is needed.

ACKNOWLEDGMENTS

It is a pleasure to thank Dr. D. H. Douglass, Jr. for suggesting this problem and for providing valuable help and encouragement throughout the entire work. I have benefited greatly from discussions with Dr. B. I. Miller, Dr. J. F. Koch, Dr. M. G. Priestley, Dr. V. Rehn, Dr. R. W. Stark, and Dr. M. Strongin on various experimental aspects of this work. I have also found fruitful theoretical discussions with Dr. K. H. Bennemann, Dr. P. E. Bloomfield, Dr. K. Maki, and Dr. F. M. Mueller. Communication by Dr. B. D. Josephson of his unpublished results is gratefully acknowledged.

I would also like to thank Dr. R. W. Johnson for suggestions on sample preparation and A. Ware for assistance in preparing samples. I am grateful to L. Cooley for assistance in building up the experimental station and also to S. Wren for special machining. I would like to thank D. Zimmerman for design and construction of portions of the electronics. For her efforts in preparing this manuscript, I am very grateful to Mrs. Audrey L. Kisel.

This research was supported in part by the Army Research Office (Durham) and the Advanced Research Projects Agency. The use of the facilities of, and the technical assistance of the personnel of, the Low Temperature Laboratory (supported by the National Science Foundation) and the Materials Preparation Laboratory (supported by the Advanced Research Projects Agency) are gratefully acknowledged.

APPENDIX

In the experiment, we actually measure the real and imaginary parts of the reflection coefficient Γ . Plotting these on the Smith chart gives the resistance \Re/\mathfrak{z}_0 and reactance $\mathfrak{X}/\mathfrak{z}_0$ of the loaded resonator. We wish to obtain, from changes in these quantities, the changes in the superconducting surface resistance R_S and reactance X_S normalized to the normal-state resistance R_N . We may adjust the tuning so that we look at the resonant system impedance in the detuned open position, where its impedance corresponds to that of an equivalent series resonant circuit.³⁵ In this case

$$\mathfrak{z} = \Re + j\mathfrak{X} = \mathfrak{z}_0 \beta^{-1} (1 + j2Q_0\delta), \quad (\text{A1})$$

where $j = \sqrt{-1}$, the quantity \mathfrak{z}_0 is the waveguide impedance, Q_0 is the intrinsic Q of the loaded resonator, $\beta = Q_0/Q_{\text{ext}}$ is the coupling coefficient, Q_{ext} represents external losses, and $\delta = (\omega - \omega_0)/\omega$ is called the frequency-tuning parameter, with ω the signal klystron frequency and ω_0 the resonant frequency of the loaded resonator.

Application of a magnetic field to the superconducting sample causes its surface impedance to change, and thus the impedance of the loaded resonator changes.

For the change in resistance of the loaded resonator $\Delta\mathcal{R}=\mathcal{R}(H)-\mathcal{R}(0)$, we have

$$\Delta\mathcal{R}/\partial_0=\Delta\beta^{-1}=Q_{\text{ext.}}(\omega L)^{-1}\Delta R_S, \quad (\text{A2})$$

since $Q_{0S}=\omega L/(R_S+R_D)$, where R_D is an equivalent resistance representing the dielectric losses which do not change with H . The quantity L is an equivalent series-circuit inductance. The change in R_S due to a shift in ωL is negligible. For critical coupling at $H=0$, we have $\beta=1$, i.e., $Q_{\text{ext.}}=Q_{0S}$, so that for (A2) we obtain

$$\Delta\mathcal{R}/\partial_0=\Delta R_S/(R_S+R_D). \quad (\text{A3})$$

Since we are interested in changes in R_S normalized to R_N , we rewrite (A3) as

$$\frac{\Delta R_S}{R_N} = \frac{\Delta\mathcal{R}}{\partial_0} \frac{R_S+R_D}{R_N}. \quad (\text{A4})$$

We define $f=R_D/R_N$. Also we have

$$Q_{0N}=\omega L/(R_N+R_D).$$

Assuming no frequency change between normal and superconducting states—which, to a good approximation, is what is observed in this case—we obtain the ratio

$$\frac{Q_{0N}}{Q_{0S}} = \frac{R_S+R_D}{R_N+R_D},$$

or $R_S+R_D=R_N(1+f)Q_{0N}/Q_{0S}$. This we may write as

$$R_S/R_N=(1+f)Q_{0N}/Q_{0S}-f, \quad (\text{A5})$$

and with (A4) we obtain

$$\frac{\Delta R_S}{R_N} = \frac{\Delta\mathcal{R}}{\partial_0} (1+f) \frac{Q_{0N}}{Q_{0S}}. \quad (\text{A6})$$

For the change in reactance of the loaded resonator

$\Delta\mathfrak{X}=\mathfrak{X}(H)-\mathfrak{X}(0)$, we have

$$\Delta\mathfrak{X}/\partial_0=\Delta(2Q_0\delta/\beta)=(-2L\Delta\omega_0)Q_{\text{ext.}}(\omega L)^{-1}. \quad (\text{A7})$$

We now show that $\Delta X_S=-2L\Delta\omega_0$ by considering an equivalent series RLC circuit. The reactance of such a circuit is given by $\mathfrak{X}=\omega L-(\omega C)^{-1}$, where C is an equivalent capacitor. Varying \mathfrak{X} we get $\Delta\mathfrak{X}=\omega\Delta L+\omega^{-1}C^{-2}\Delta C=L[\omega(\Delta L/L)+\omega^{-1}(LC)^{-1}(\Delta C/C)]$. In the experiment, only the sample reactance is changed by applying H , so that $\Delta L=\Delta L_S$, $\Delta C=\Delta C_S$, and $\Delta\mathfrak{X}=\Delta X_S$. The frequency change is small compared to the resonant frequency, so that $\omega\approx\omega_0$. We have then

$$\Delta X_S=L[\omega_0(\Delta L_S/L)+\omega_0(\Delta C_S/C)], \quad (\text{A8})$$

since $\omega_0^2=(LC)^{-1}$. Varying this expression for ω_0^2 , we get

$$2\Delta\omega_0=-\omega_0(\Delta L_S/L)-\omega_0(\Delta C_S/C). \quad (\text{A9})$$

Substituting (A9) into (A8) yields

$$\Delta X_S=-2L\Delta\omega_0, \quad (\text{A10})$$

so that from (A7) we have

$$\Delta\mathfrak{X}/\partial_0=(\Delta X_S)Q_{\text{ext.}}(\omega L)^{-1}=\Delta X_S/(R_S+R_D). \quad (\text{A11})$$

Proceeding in the same manner as for the resistance, we obtain

$$\frac{\Delta X_S}{R_N} = \frac{\Delta\mathfrak{X}}{\partial_0} (1+f) \frac{Q_{0N}}{Q_{0S}}. \quad (\text{A12})$$

We find the value of f from the requirement $R_S/R_N=0$ at $t=0$ so that

$$(1+f)Q_{0N}/Q_{0S}=f \quad \text{or} \quad f=Q_{0N}(Q_{0S}-Q_{0N})^{-1}.$$

In this experiment we found $f=0.99$, assuming that Q_{0N} was independent of t and H in the ranges in which we were working and that Q_{0S} at $t=0.225$ was practically the same as it would be at $t=0$. In other words, we assume that $R_S\approx 0$ at $t=0.225$ with $H=0$. The values of Q_{0S} and Q_{0N} are obtained as described in Sec. III.